2014 IEEE International Conference on Robotics & Automation (ICRA)
Hong Kong Convention and Exhibition Center
May 31 - June 7, 2014. Hong Kong, China

Hovering of MAV by Using Magnetic Adhesion and Winch Mechanisms

Kazuaki Yanagimura, Kazunori Ohno, Yoshito Okada, Eijiro Takeuchi, and Satoshi Tadokoro

***Abstract*— We propose a method by which a micro air vehicle (MAV) can hover without propulsion power. In this paper, we describe the design of a magnetic adhesion mechanism and a winch mechanism for an MAV that is used to perform search operations inside buildings. An MAV equipped with these mechanisms can adhere to an iron ceiling and search for a long time from an appropriate position. We designed a magnetic adhesion mechanism with an adhesion force of over 20 N. The magnetic adhesion mechanism comprises a magnet, dual coil springs, and a switching mechanism. Using models of MAV and the adhesion mechanism, we determined the parameters of the mechanism. The magnetic adhesion mechanism can be detached easily by a force less than the magnetic adhesion force. The winch mechanism comprises a structure to retriev the adhesion mechanism, a strong, lightweight tether and a servo-motor that produces enough torque to lift the MAV by the tether. We confirmed that the MAV can hover without propulsion power by using these mechanisms.**

I. INTRODUCTION

We have researched a micro air vehicle (MAV) that can search inside damaged buildings. MAVs can enable us to search places that are difficult for people to search, such as plumbing at high positions in industrial plant or in and around the Fukushima Daiichi nuclear power plant. Actually, a Global Hawk unmanned aircraft was used to search outside the Fukushima Daiichi nuclear power plant. One paper reported that the combination of an unmanned ground vehicle and MAV was effective for searching damaged buildings[1]. MAVs are appropriate for searching disaster sites.

A battery powered MAV is appropriate for searching inside damaged buildings because it is smaller and safer than an MAV driven by petrol. However, its payload is limited, and its flight time is from 10 to 15 minutes. The flight time decreases to half when the MAV hovers. We seek to increase the flight time.

Hovering mode consumes much energy. Electrical devices mounted on an MAV do not require as much energy as the propulsion power. Therefore, we consider that the flight time can be extended by reducing the power required for hovering. Adhesion to a wall or ceiling is one solution for hovering without propulsion power. In the present paper, we propose a method by which an MAV hovers and observe without propulsion power by using a magnetic adhesion mechanism and a winch mechanism. The proposed method is similar to spiders.

Several researchers have studied MAVs with mounted adhesion mechanisms. Yong Liu developed an MAV like

*This work was not supported by any organization

All authors are with Graduate School of Information Sciences, Tohoku University, Sendai, Japan. Kazuaki Yanagimura: yanagimura@rm.is.tohoku.ac.jp

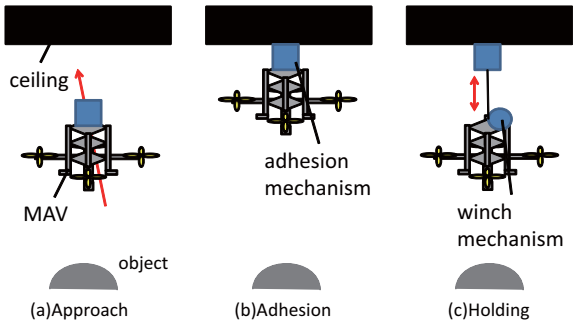

Fig. 1. Adhesion task

resembles a bat in that it can adhere to a ceiling and detach arbitrarily by using a negative pressure (suction) mechanism. James F. Roberts developed an MAV with a mounted magnet. With the help of the magnet, it can adhere to a ceiling without consuming power, and it can arbitrarily switch between adhering and detaching. By referencing these related works, we propose a magnetic adhesion mechanism. In addition, we have added a new function by which an MAV approaches a target object from above by using a winch mechanism.

Many approaches have been proposed for adhering to walls and ceilings: negative pressure[4], [5], magnetic adhesion[6], [7], micro spines[8], electrical adhesion[9], [10], adhesive pad[11], [12], and biomimetics[13], [14]. Our target environment is industrial plants and damaged buildings. Therefore, we require our adhesion method to fulfill the following criteria.

1) Low power consumption ($\simeq$0 W) and strong adhesion force (>20 N)
2) Light weight (<100 g)
3) Repeated use of adhesion mechanism
4) Minimal damage to target objects
5) Adhesion to various materials

We compared each adhesion method on the basis of the abovementioned criteria. Table. I lists the comparison results. Magnetic adhesion fulfilled almost all the criteria.

Therefore, we selected magnetic adhesion for our adhesion mechanism. Although magnet can adhere only to ferromagnetic substances such as iron and steel, we considered that magnetic adhesion mechanism would be useful because there is usually much iron and steel in industrial plants and damaged buildings.

In this paper, we propose a small and light magnetic adhesion and a winch mechanism for an MAV. In Section II, we explain the process that a hovering MAV performs the task of observation. In Sections III and IV, we describe mechanisms mounted on an MAV. In Section V, we show

TABLE I

COMPARISON OF ADHESION METHODS (++:FAVORABLE, +:LITTLE FAVORABLE, -:SLIGHTLY UNFAVORABLE, −−:UNFAVORABLE)

adhesion method	low power consumption	adhesion force for weight	continuous using	less danger to surroundings	attaching to diverse substance
negative pressure[4], [5]	-	++	++	+	++
magnetic adhesion[6], [7]	++	++	++	++	−−
micro spines[8]	++	+	++	-	+
electrical adhesion[9], [10]	+	-	+	-	++
adhesive pad[11], [12]	++	+	-	+	-
biomimetics[13], [14]	++	-	-	+	-

how an MAV can adhere to a ceiling, lower itself on a tether, and observe objects.

II. TARGET OBSERVATION USING MAV WITH MAGNETIC ADHESION AND WINCH MECHANISM

A. Outline of target task

We observed target objects using an MAV that can hover without propulsion power. Figure 1 shows the outline of our target task. First, the MAV flies and approaches the ceiling (Fig. 1(a)). Then, it adheres to the ceiling by using an adhesion mechanism (Fig. 1(b)). After adhering to the ceiling, the MAV stops its rotors and moves to an arbitrary height by rolling the tether up or down. A winch mechanism is used to unroll and roll up the tether. After performing the observation, the MAV rolls up the tether and retrieves the adhesion mechanism (Fig. 1(c)). By repeating these processes, the MAV can adhere to a ceiling, make observations, and then fly to a new location. Hovering without propulsion power can extend the search time.

We propose an adhesion mechanism that can adhere and detach repeatedly. In addition, we propose a winch mechanism that can unroll and roll up the tether and switch the adhesion mechanism between adhesion and release modes by using a single motor mounted on the MAV. The adhesion mechanism does not contain any actuators. Therefore, the winch mechanism does not unroll and roll up any electric cables. This characteristic can prevent electrical cables from breaking, and it allows us to use a thin cable.

B. MAV and requirement of adhesion mechanism

We used a quadrotor made by Ascending Technology as the MAV. Its weight is 1.27 kg, and its payload is 330 g. Its flight time is 15 min at maximum weight. The adhesion and winch mechanisms need to support the weight; therefore, the target adhesion force must be greater than 20 N. Furthermore, weight of the mechanisms must be less than the payload of the MAV (330 g). Therefore, the total weight of the mechanism should be under 100 g. We designed these mechanisms by fulfilling these target values.

III. ADHESION MECHANISM

A. Outline of adhesion mechanism

We designed a magnetic adhesion mechanism mounted on an MAV. A strong neodymium magnet can generate an adhesion force greater than 20 N. However, detaching it requires an even stronger force. We seek to detach the adhesion mechanism with a weaker force. An internally balanced magnetic unit (IB magnet[15]) is one solution. The IB magnet adheres to ferromagnetic materials by using a magnet and is detached by less force because of the elastic force of a spring. By using an mechanism of IB magnet, we developed a magnetic adhesion mechanism with an adhesion force greater than 20 N and release force that is less than 20 N. In addition, the switching between these modes is done using the winch mechanism.

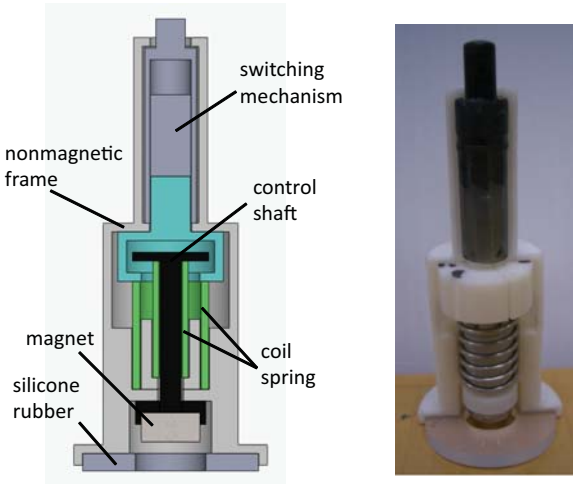

Fig. 2. Developed magnetic adhesion mechanism

The structure of the magnetic adhesion mechanism is described in Section III-B. We determined that our magnet generates sufficient adhesion force using the MAV model described in Section III-C. We formularize the elastic force of the magnetic adhesion mechanism in Section III-D. From the models, an appropriate pair of coil springs was selected. In Section III-E, we evaluate the developed adhesion mechanism.

B. Composition of adhesion mechanism

Figure 2 shows the developed magnetic adhesion mechanism. It comprises a control shaft, dual coil springs, a switching mechanism, a magnet, and a silicon rubber bumper.

Figures 3 and 4 show the adhering and detaching motion of the developed adhesion mechanism. The switching mechanism alternates its operation mode. By pushing the switch, the MAV can adhere to a ceiling and then detach. Because of the dual coil springs inside the adhesion mechanism, the MAV can detach with less force than magnetic adhesion

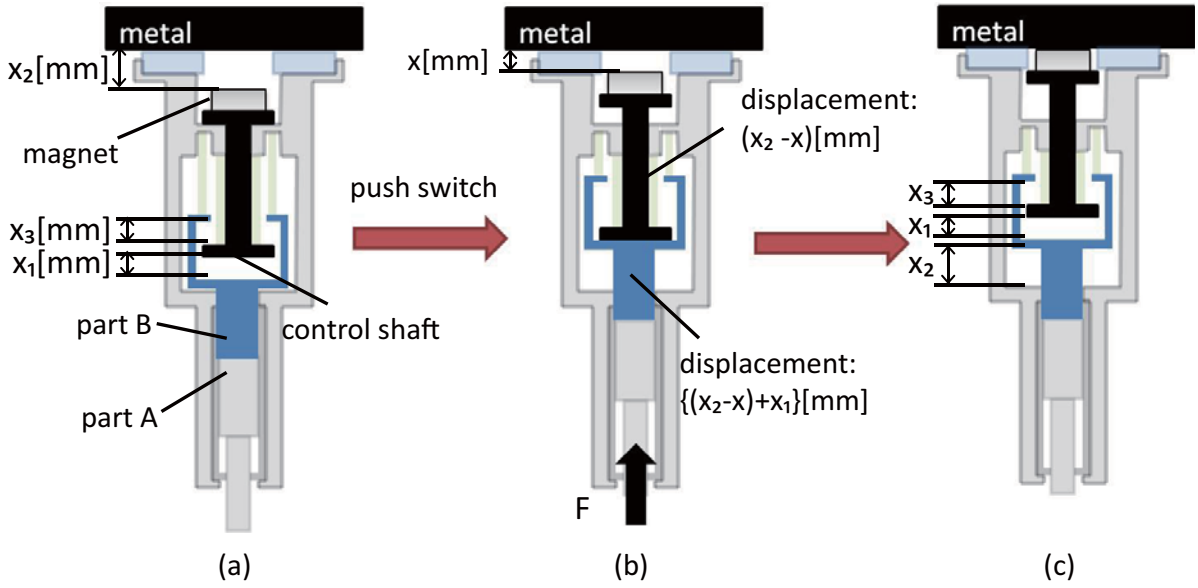

Fig. 3. Flow of adhering motion

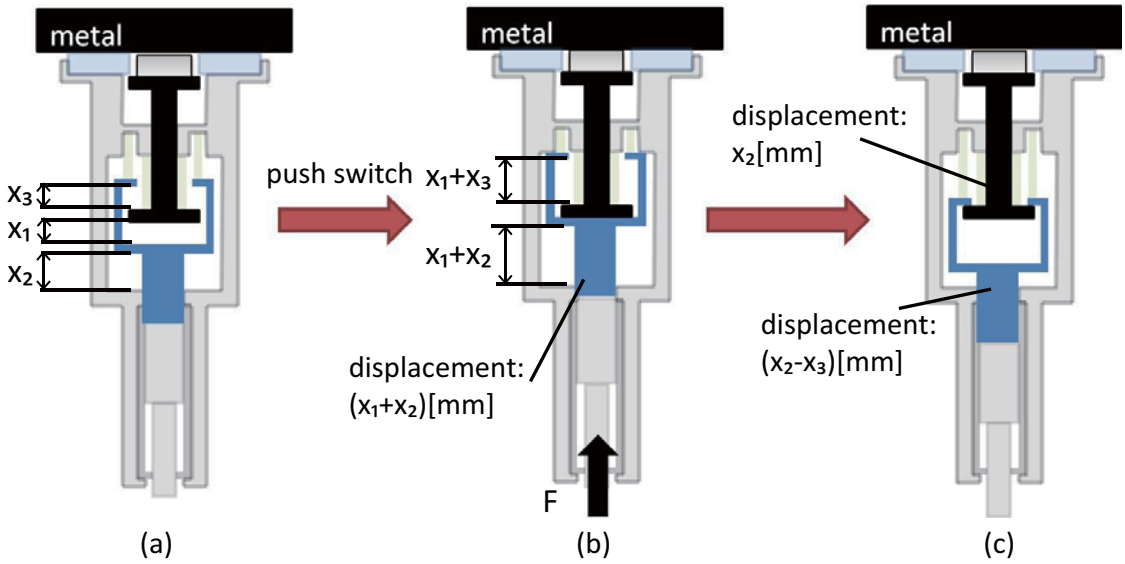

Fig. 4. Flow of detaching motion

force.

When the mechanism adheres to a ceiling, part A inside the switching mechanism moves to the high position (Fig. 3(b)). It cannot move to a lower position. An elastic force from the coil springs is applied to the control shaft. However, the magnet remains adhered to the surface because the elastic force is less than magnetic adhesive force (Fig. 3(c)).

When the mechanism is detached, the part inside the switching mechanism moves to the low position. By pushing the switch and moving the part to a higher position, it can then be moved to a lower position (Fig. 4(b)). The sum of the elastic forces of dual coil springs is applied to the control shaft (Fig. 4(c)). If the sum of elastic forces is stronger than the magnetic adhesive force, the magnet inside the adhesion mechanism is detached. After detaching, the adhesion mechanism returns the state shown in Fig. 3(a).

Therefore, the MAV can adhere and detach repeatedly. In addition, to increase the coefficient of friction, we integrated a silicon rubber bumper into the mechanism. To lighten it, all components are made of acrylonitrile-butadiene-styrene (ABS) plastic, except the magnet, spring, and silicone rubber bumper.

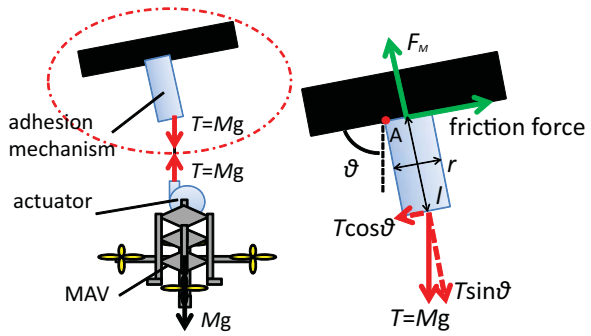

(a) (b)

Fig. 5. Dynamic model of MAV and adhesion mechanism

C. Modeling adhesion mechanism

We need to choose a magnet such that the adhesion mechanism is not detached by lateral forces or the tension in the tether. We determined whether the chosen magnet has sufficient adhesion force by modeling.

Figure 5 shows a dynamic model of the adhesion mechanism. The relationship between the force between the MAV and the adhesion mechanism is shown in Fig. 5(a). Figure 5(b) shows an enlarged view of the adhesion mechanism - the part surrounded by a red dashed line in Fig. 5(a). We modeled the adhesion mechanism with the following parameters: weight of MAV M [kg], magnetic adhesion force F_M [N], coefficient of friction μ, diameter of adhesion mechanism r [mm], and distance from the object surface to the connecting point of the tether l [mm]. From the model in Fig. 5(b), the formula for dynamic balance and moment balance is derived as follows:

$$F_M > Mg\sin\theta \tag{1}$$

$$F_M > Mgsin\theta/\mu + Mg\cos\theta \tag{2}$$

$$F_M > Mg(2l\cos\theta/r + \sin\theta) \tag{3}$$

The adhesion mechanism must satisfy the above formulas. We chose a magnet with F_M = 30 N from available magnets. The parameters for dimensions and materials are calculated in reference to parts used as follows: μ = 0.9, r = 30mm, l = 5 mm. Figure 6 shows the relationship between the angle in Eqs. (1-3), θ, and the required adhesion force, F_M. Our adhesion mechanism has enough adhesion force to adhere to a ceiling at an angle of 0°-90° because it is designed to fulfill the above mentioned parameters.

D. Formularization of elastic force inside mechanism

We modeled the elastic force inside the adhesion mechanism to calculate the force required to actuate the switching mechanism by using the elastic modulus of the dual coil springs and dimension of adhesion mechanism. Figure 3(a) shows the distance between each item for modeling. The distances were derived as follows: displacement for converting the adhesion mechanism from adhering to detaching, x_1;

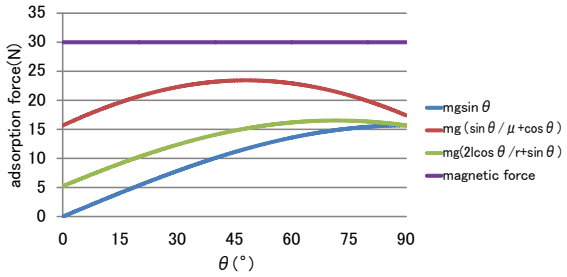

Fig. 6. Relationship between angle and adhesion force

difference of displacement of the part inside the switching mechanism between adhering and detaching, x_2; distance where there is no contact between the control shaft and part A, x_3. In addition, the elastic modulus of the outside spring is k_1, and that of the inside spring is k_2.

The position of the control shaft and part A in Fig. 3 are related to the elastic force of the coil springs. The state in Fig. 3(a) is defined as the initial state. The displacement of part A is equal to the displacement of the outside coil spring, and the displacement of the control shaft is equal to the displacement of the inside coil spring.

*a) **Adhering**:* Figure 3 shows the motion of adhering. We formulized the elastic force in the case where part A contacts the control shaft. The distance between the magnet and the surface of the object is x[mm].

In Fig. 3, the pushing force to move the control shaft to the position of x [mm] from object surface is F, and the attractive magnetic force is $F_M(x)$. We prepared in advance a table that describes the relationship between magnet adhesion force $F_M(x)$ and the distance between the magnet and the object. When the adhesion mechanism is adhering, the displacement of part A is $(x_2 - x) + x_1$ [mm], and the displacement of the control shaft is $(x_2 - x)$ [mm].

If the magnetic adhesion force is less than the elastic force of the inside coil spring, the pushing force F_1 is calculated as follows:

$$F_1 = k_1(x_1 + x_2 - x) + k_2(x_2 - x) - F_M(x) \tag{4}$$

In contrast, if the magnetic adhesion force is higher than the elastic force of the inside coil spring, the magnet adheres to the object so that the control shaft does not contact part A. The elastic force of the inside coil spring does not affect the pushing force F. Therefore, F_2 is calculated as below:

$$F_2 = k_1(x_1 + x_2 - x) \tag{5}$$

The force to push the switching mechanism is calculated by $\max\{F_1, F_2\}$.

*b) **Detaching**:* Figure 4 shows the motion of the detachment of adhesion mechanism. We need to displace part A to the position shown in Fig. 4(b) to detach it. The elastic force of the inside coil spring is not considered because it is canceled by the magnetic adhesion force. The pushing force needed to detach the adhesion mechanism F is calculated as

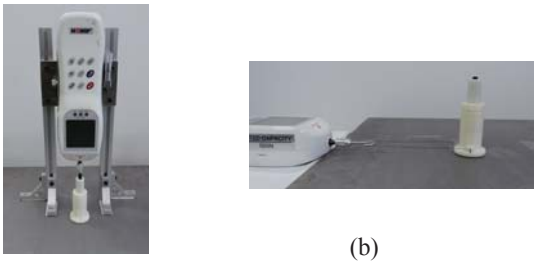

(a) (b)

Fig. 7. Performance evaluation experiment

$$F = k_1(x_1 + x_2) \tag{6}$$

When the magnet is detached, the displacement of the control shaft is x_2[mm], and the displacement of part A is $(x_2 - x_3)$ [mm].

We need to satisfy Eq. (7) below so that the magnet is not detached during the adhering motion, as shown in Fig. 3, and it is detached after the detaching motion, as shown in Fig. 4.

$$k_2 x_2 < F_M < k_1(x_2 - x_3) + k_2 x_2 \tag{7}$$

We determined the elastic modulus, k_1, k_2 that satisfies the above formula.

E. Evaluation of adhesion mechanism

We evaluated the adhesion mechanism designed in Sections III-C and III-D. Figure 7 shows the experimental equipment. The object is to adhere to a plate of S45C with a thickness of 3 mm. We measured forces five times in each case. We evaluated the elastic force, which is calculated in Section III-D, and we chose a combination of coil springs from available springs. Additionally, we evaluated whether the adhesion mechanism performed as described in Section III-C.

The dimensions of the adhesion mechanism are as follows: x_1 = 2.5 mm, x_2 = 6.0 mm, x_3 = 2.0 mm. The combinations of dual coil springs we used are (k_1,k_2) = (1.0,4.5) [N/mm], (1.4,4.1) [N/mm], (2.9,2.9) [N/mm]. Tables II and III list the experimental results. The pushing force to adhere the adhesion mechanism is between 20 N and 26N. It is smaller than the magnetic force 30 N. The pushing force to detach the adhesion mechanism is approximately 10 N in the first two combinations; for the third combination, it equal to the magnetic adhesion force comparison.

In all cases in Tables II and III, the measured value was higher than the theoretical value. We think this was due to friction between the parts, as well as the extra elastic forces of the coil springs due to dimensional error. Though the error exists, we can estimate the force to actuate the mechanism substantially in the case of (k_1,k_2) = (1.4,4.1) [N/mm], (2.9,2.9) [N/mm]. In the case of (k_1,k_2) = (1.0,4.5) [N/mm], the adhesion mechanism could not adhere owing to the extra elastic force of the inside coil spring, so the error was greater than in the other result. From measurements, we chose the combination of (k_1,k_2) = (1.4,4.1) [N/mm].

TABLE II

PUSHING FORCE TO ADHERE

k_1 (N/mm)	k_2 (N/mm)	theoretical value (N)	measured value (N)	error (N)
1.0	4.5	20.7	20.0	-0.7
1.4	4.1	21.7	22.7	+1.0
2.9	2.9	26.8	28.1	+1.3

TABLE III

PUSHING FORCE TO DETACH

k_1 (N/mm)	k_2 (N/mm)	theoretical value (N)	measured value (N)	error (N)
1.0	4.5	8.5	15.1	+6.6
1.4	4.1	11.9	13.3	+1.4
2.9	2.9	24.7	26.0	+1.3

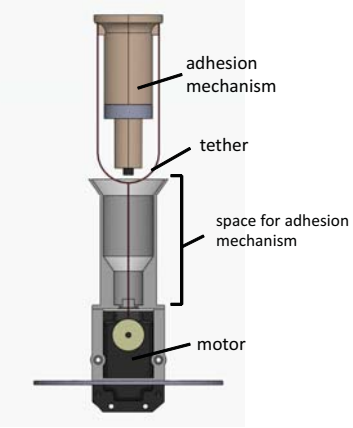

Fig. 8. Composition of winch mechanism

Furthermore, we evaluated the adhesion mechanism into which the above combination of coil springs is built, for adhesion force, coefficient of friction, and moment. We pulled the adhesion mechanism vertically and horizontally, and measured the force at the time it detached.

The adhesion force was measured to be 31.28 ($\pm$0.60) N, and the coefficient of friction was measured to be 0.87 ($\pm$0.01). In addition, the adhesion mechanism was not detached by moment. On the basis of these results, we showed that the developed mechanism meets the performance requirements described in Section III-C.

IV. WINCH MECHANISM

A. Composition of winch mechanism

Figure 8 shows the developed winch mechanism. It consists of a tether, a reel, and an actuator. Figure 9 shows the motion of the winch mechanism. When the adhesion mechanism adheres to the ceiling, the MAV moves to an appropriate height for carrying out observation by using the winch mechanism (Fig. 9(a)). The MAV retrieves the adhesion mechanism by rolling up the tether and pushing the switch for the adhesion mechanism (Fig. 9(b)). After the retrieval, the MAV can fly (Fig. 9(c)). The adhesion and release modes can be actuated using a single motor.

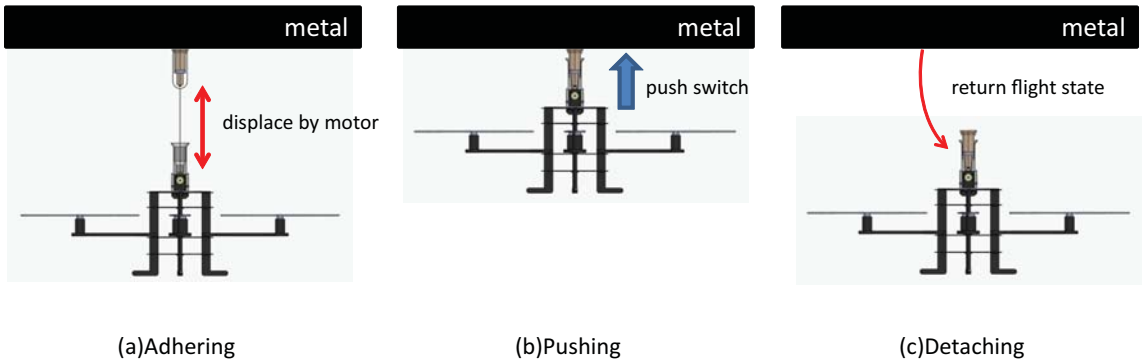

Fig. 9. Winch mechanism tasks

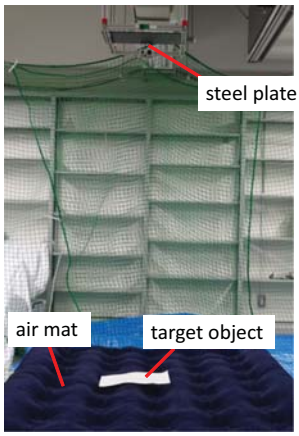

Fig. 10. Experimental equipment

Fig. 11. MAV with integrated adhesion and winch mechanism

A polyethylene tether is used because it is light, thin, and strong enough to support the MAV. An actuator is needed to generate a force greater than 20 N for lifting the MAV. Therefore, the target torque is greater than 20 Ncm because the radius of reel is 10 mm. We selected 60 rpm as the reel speed. From these target values, we selected a servomotor made by Dynamixel as the actuator.

Its maximum torque is 260 Nm, maximum rotation speed is 126 rpm, weight is 67 g, and maximum power consumption is 29 W. This servomotor can repeatedly generate strong forces because it has metal gears. Moreover, the servomotor contains a controller and is easily controlled from an onboard PC.

B. Evaluation winch mechanism

We show whether the MAV can move to an arbitrary height using the winch mechanism. In addition, we measured the power consumption to compare it with power consumption of a hovering MAV, and we validated the improvement in power consumption. Figure 10 shows the experimental equipment. We connected the tether to the upper structure and had the MAV change its height using the winch mechanism. We measured the power consumption while the MAV changed its position at speeds of 3.3 cm/s, 6.6 cm/s, and 13.2 cm/s (maximum speed).

Power consumption was measured to be 3.25 W at 3.3 cm/s, 4.82 W at 6.6 cm/s, and 2.53 W at 13.2 cm/s. Then, we calculated the power consumption of the hovering MAV. The electric energy capacity of the battery mounted on the MAV is 66.6 Wh, and the flight time of the MAV is 15 minutes.

On the basis of these specifications, we calculated that power consumption of flying the MAV to be 266.4 W. Moreover, the MAV consume approximately twice as much power when it is hovering as when it is flying, so we calculated power consumption for hovering the MAV to be 532.8 W. The maximum power consumption of the winch mechanism is less than 1% of power consumption of a hovering MAV. On the basis of this comparison it was concluded that the winch mechanism consumes much less electric power than a hovering MAV.

V. Adhering and Rolling Up Experiment Using MAV

We integrated the magnetic adhesion mechanism described in Section III and the winch mechanism described in Section IV into the MAV. We evaluated whether it could achieve the target task.

The integrated MAV is shown in Fig. 11, and the system on the MAV is shown in Fig. 12. As shown in Fig. 12, we can maneuver using Atomboard by radio communication

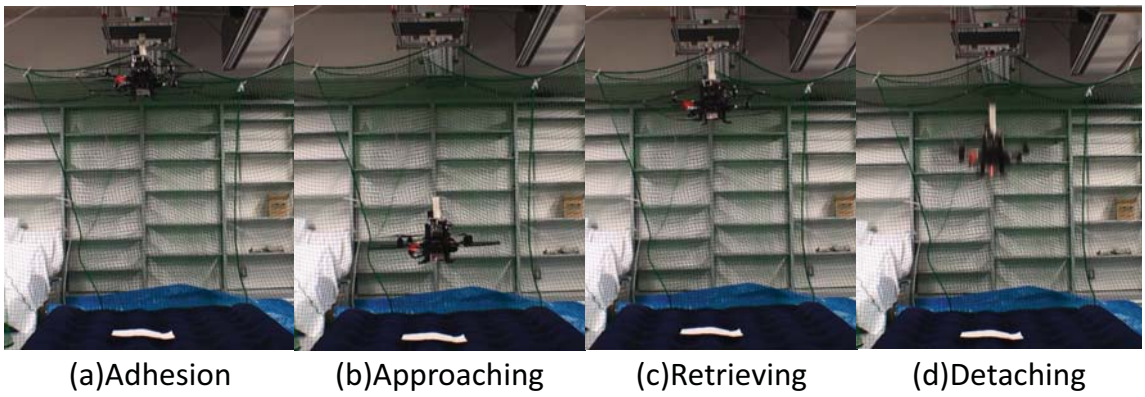

Fig. 13. Motion of MAV

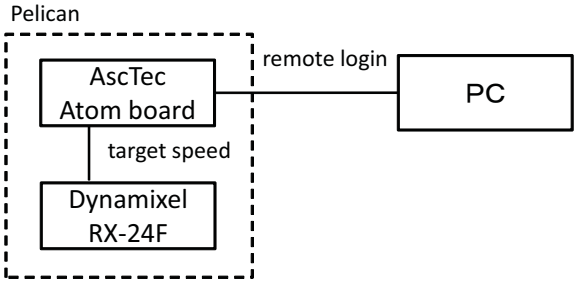

Fig. 12. system

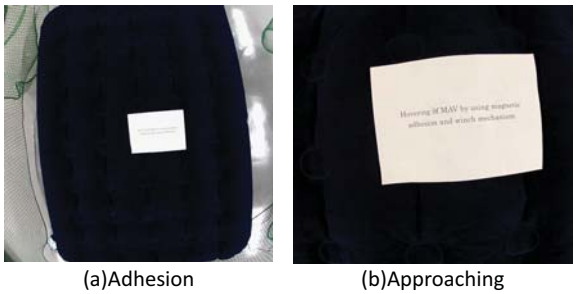

Fig. 14. Camera view

and control the actuator by sending the target speed from Atomboard. We mounted a small camera at bottom of MAV.

The MAV adhered to a steel plate and moved vertically within a roughly cubic space of 3 m $\times$ 3 m $\times$ 2.4 m (shown in Figure 10). It was attached to the ceiling by hand. To ensure safety during the experiment, we placed a net around the perimeter of the experimental area and put air mattresses on the floor to prevent the MAV from being damaged when it fell after detaching the adhesion mechanism. The adhering object, a steel plate with a thickness of 3 mm, was set near the ceiling of the room at a distance of 1700 mm from the floor.

The motion of our MAV is shown in Figure 13. MAV adhered to a ceiling, and detached the adhesion mechanism. The camera view is shown in Figure 14. In camera view, MAV observe an object nearly.

VI. Discussion

We developed an adhesion mechanism and a winch mechanism and installed them on an MAV (Fig. 11). The total weight of mechanisms is 148.6g. Though it is higher than required parameter, the adhesion and winch mechanisms are light enough to mount on MAV. As future works, We would like to lighten them.

We confirmed that the MAV adhered to a ceiling, approached an object from above, and detached the adhesion mechanism (in Section V). The adhesion mechanism adhered to the ceiling with the angle between the ceiling and the adhesion mechanism at 15°. We confirmed that the mechanism met our requirements in Sections III and IV.

The MAV sometimes failed to adhere to the ceiling when it approached the ceiling too fast. The developed adhesion mechanism by us used a silicon rubber ring for absorbing the impulse force and increasing the friction coefficient. However, it was not sufficient. We need to improve the adhesion mechanism for the impulse force.

We observed that the MAV rotated slowly around its yaw angle while the MAV changed its height using the winch mechanism. We need to cope with the rotation. The rotation motion of MAV can be prevented by using the rotors. The images captured by the onboard cameras will rotate according to the yaw rotation. These are new research topics.

We used a magnet as the adhesion method. However, various other adhesive materials also exist. We need to develop other adhesion mechanisms that can adhere to nonmagnetic materials. This will be our future work.

VII. Conclusions

This paper proposed a method by which an MAV adheres to a ceiling by using an adhesion mechanism to hover without propulsion by hanging from the ceiling. We designed a magnetic adhesion mechanism that can be detached by operating a switch, and a winch mechanism that can unroll and roll up a tether for the MAV. The experiment with the developed MAV-mounted mechanisms showed that an MAV can adhere to steel and hover at an arbitrary distance from a ceiling.

REFERENCES

[1] Nathan Michael, Shaojie Shen, Kartik Mohta, Yash Mulgaokar, Vijay Kumar, Keiji Nagatani, Yoxhito Okada, Seiga Kiribayashi, Kazuki Otake, Kazuya Yoshida, Kazunori Ohno, Eijiro Takeuchi, and Satoshi Tadokoro, "Collaborative Mapping of an Earthquake-Damaged Building via Ground and Aerial Robots", Field and Service Robotics, 2013

[2] Yong Liu, Heping Chen, Zhenmin Tang, and Guoxin Sun, "A Bat-like Switched Flying and Adhesive Robot", IEEE International Conference on Cyber Technology in Automation, Control and Intelligent Systems, pp.92-97, 2012

[3] James F. Roberts, Jean-Christophe Zufferey, and Dario Floreano, "Energy Management for Indoor Hovering Robots", IEEE/RSJ International Conference on Intelligent Robots and Systems Acropolis Convention Center, pp1242-1247, 2008

[4] Yusuke OTA, Toru KUGA, and Kan YONEDA, "Deformation Compensation for Continuous Force control of a Wall Climbing Quadruped with Reduced-DOF", IEEE International Conference on Robotics and Automation, pp.468-474, May 2006

[5] Shanqiang Wu, Lijun Wu, and Tao Liu, "Design of a Sliding Wall Climbing Robot with a Novel Negative Adsorption Device", IEEE International Conference on Ubiquitous Robots and Ambient Intelligence, pp.97-100, 2011

[6] Zeliang Xu and Peisun Ma, "A wall-climbing robot for labelling scale of oil tank's volume", Robotica, Vol.20, pp.209-212, 2002

[7] Samuel Jensen-Segal, Steven Virost, and William R. Provancher, "ROCR: Dynamic vertical wall climbing with a pendular two-link mass-shifting robot", IEEE International Conference on Robotics and Automation, pp.3040-3045, 2008

[8] Aaron Parness, Matthew Frost, Nitish Thatte, and Jonathan P. King, "Gravity-Independent Mobility and Drilling on Natural Rock Using Microspines", IEEE International Conference on Robotics and Automation, pp.3437-3442, 2012

[9] Harsha Prahlad, Ron Pelrine, Scott Stanford, John Marlow, and Roy Kornbluh, "Electroadhesive Robots - Wall Climbing Robots Enabled by a Novel, Robust, and Electrically Controllable Adhesion Technology", IEEE International Conference on Robotics and Automation, pp.3028-3033, 2008

[10] Huan P. Diaz Tellez, Jeff Krahn, and Carlo Menon, "Characterization of Electro-adhesives for Robotic Applications", IEEE International Conference on Robotics and Biomimetics, pp.1867-1872, 2011

[11] Ozgur Unver, Ali Uneri, Alper Aydemir, and Metin Sitti, "Geckobot: A Gecko Inspired Climbing Robot Using Elastomer Adhesives", IEEE International Conference on Robotics and Automation, pp.2329-2335, 2006

[12] Michael P. Murphy, William Tso, Michael Tanzini, Metin Sitti, "Waalbot: An Agile Small-Scale Wall Climbing Robot Utilizing Pressure Sensitive Adhesives", IEEE/RSJ International Conference on Intelligent Robots and Systems, pp.3411-3416, 2006

[13] Kellar Autumn, "Properties, Principles, and Parameters of the Gecko Adhesive System", 2006

[14] Sangbae Kim, Matthew Spenko, Salomon Trujilo, Barrett Heyneman, Virgilio Mattoli, and Mark R. Cutkosky, "Whole body adhesion: hierarchical, directional and distributed control of adhesive forces for a climbing robot", IEEE International Conference on Robotics and Automation, pp.1268-1273, 2007

[15] Shigeo Hirose, "A New Design Criterion in Robotic Mechanism (Prevention of Negative Power Consumption)", IEEE/RSJ International Conference on Intelligent Robots and Systems, pp131-135, 1993